JOURNAL OF CATALYSIS 120, 118–136 (1989)

The CO/H_2 Reaction on Rh/Al_2O_3

I. Steady-State and Transient Kinetics

ANGELOS M. EFSTATHIOU AND CARROLL O. BENNETT

Department of Chemical Engineering, University of Connecticut, Storrs, Connecticut 06268

Received August 3, 1988; revised September 29, 1988

Various hydrogen titrations yield the surface composition of Rh/Al_2O_3 during the CO/H_2 reaction at temperatures in the range 180–260°C. There is a very small amount of active carbon C_α, 0.02–0.06 monolayer, and 0.70–0.98 monolayer of CO on the metal surface. The coverage of H is low. Also present are inactive carbon C_β on the metal and formate species on the support. The surface coverages are consistent with the observed steady-state kinetics, which result in methane as the predominant product. Although the rate-limiting step may be the dissociation of surface CO, it is found that the reaction sequence passes through a small coverage of highly active surface carbon C_α. © 1989 Academic Press, Inc.

INTRODUCTION

For supported Rh catalysts, the effects of changes of support or promoter on catalytic activity and selectivity for the H_2/CO reaction have been studied by many authors (*1–10*). Although Rh/Al_2O_3 is essentially a methanation catalyst, rhodium supported on MgO or La_2O_3 can be a selective catalyst to CH_3OH, C_2H_5OH, and CH_3CHO depending on the particular formulation at 1 atm total pressure (*1, 2*). In these reports the catalysts have been characterized and various kinetic, infrared, and other spectroscopic studies have been performed. Since understanding these phenomena would be facilitated by a knowledge of the state of the surface of the metal and the support during reaction, we have initiated a series of investigations of these matters by transient and transient isotopic methods. The intent is to study the effect of various supports on the kinetics of the CO/H_2 reaction and on the surface state of the Rh during catalysis. As a base case we consider the reaction over 5% Rh/Al_2O_3 in the present work. The coverage vs time on stream in CO/H_2 of the various carbon-containing species during reaction at 180°C has already been obtained (*11*). In that study the catalyst characterization and the experimental methods have been described. In general the methods are similar to those used to study the H_2/CO reaction over Ni/Al_2O_3 (*12, 13*).

For Rh/Al_2O_3, Erdohelyi and Solymosi (*14*) have studied the disproportionation of CO to give CO_2 and surface carbon by the TPR technique. Infrared spectroscopy has been extensively used to study the modes of CO adsorption as influenced by the adsorption temperature and other variables (*15–21*). For the large metal particles of the catalyst used here, no twin carbonyl adsorbed species are expected under synthesis conditions (*22*). However, Solymosi *et al.* (*9, 23*) have found that formate species are formed from H_2/CO on the alumina surface of Rh/Al_2O_3, and we shall need to take into account these results in the interpretation of our transient data.

The oxidation/reduction history of the Rh/Al_2O_3 has a striking effect on the morphology of the Rh and thus on the catalytic behavior of the catalyst (*22, 24–26*). The pretreatment and operating conditions used in this study are such that reproducible results are obtained, and catalyst deactiva-

0021-9517/89 $3.00

tion is a minor effect. Siddall *et al.* (*27*) have studied Rh/SiO_2 by transient isotopic techniques. Their results complement ours, although on SiO_2 there seems to be no accumulation of formate species (*9, 28*).

The present study is concerned with the effect of temperature and time on stream in CO/H_2 on the surface composition of the catalyst during reaction. The results are obtained principally by isothermal and temperature programed titrations by hydrogen without the use of isotopic species. However, a more complete picture of the reacting surface requires also some isotopic and other studies which are the subject of Part II of this work (*29*).

Although it is generally accepted that on Ni, Fe, or Ru the methanation reaction proceeds through a surface CH_x species, CO dissociation on Rh is much more difficult. In fact, Mochida *et al.* (*22*) propose that the rate of carbon deposition and its reactivity with hydrogen are so small that it is not an essential intermediate in the catalytic sequence. In the present study and in that which follows (*29*), we shall show that surface carbon does seem to be in the catalytic sequence, although its surface coverage is very small.

EXPERIMENTAL

Catalyst preparation. A 5.2 wt% Rh/γ–Al_2O_3 catalyst was prepared by impregnating Alon-C (Degussa) to incipient wetness (0.95 cc/g Al_2O_3) with an aqueous solution of $RhCl_3 \cdot 3H_2O$ (Aldrich Chem. Co.). The powder was dried at room temperature for 96 h followed by 2 h drying at 105°C, pressed at 2200 psia, crushed, and then screened to give 0.58- to 0.84-mm particles. For storage it was passivated by treating it under H_2 at 300°C for 3 h, then calcining it with O_2 at 400°C for 2 h.

Before the transient experiments, the freshly charged catalyst (30 mg) was first reduced with hydrogen at 350°C for 1 h, and then treated with H_2/CO mixture for 2 h at 240°C to obtain a fairly stabilized surface for subsequent experiments. From that point, an oxidation–reduction treatment with O_2 at 350°C for $\frac{1}{2}$ h followed by H_2 reduction at the same temperature for 2 h was applied prior to the experimental studies. This oxidation–reduction procedure was consistently repeated after the catalyst had been exposed to reaction mixtures for 6–8 h and this proved very efficient for maintaining the catalyst activity the same to within 2–3% at the beginning of any set of runs. After a given run the temperature was raised to 450°C under H_2 and held for 10–15 min until no methane was detectable. Then the catalyst was brought to reaction temperature under H_2. The steady-state experiments for determining the activity and selectivity of the catalyst were performed with another 35-mg sample. The fresh catalyst was first reduced for 12 h at 400°C, then brought to reaction temperature under H_2. After the catalyst had been exposed to the synthesis mixture for 2–3 h, it was then treated with H_2 at 400°C for 1 h before proceeding to the next run.

Catalyst characterization. The BET surface area of the alumina support as well as the active metal surface area were measured in a flow sorption apparatus described elsewhere (*30*). The support surface area was found to be 110 ± 5 m^2/g. The active metal surface area was obtained by extrapolating the linear part of the H_2 chemisorption isotherm at 298 K to zero pressure (*31*) and assuming $H/Rh_s = 1.0$ (*32*). The hydrogen uptake of the catalyst was found to be 30 μmol/g cat, yielding a value of 60 μmol Rh surface atoms/g of catalyst. The fraction exposed of the Rh was found to be 0.12. Assuming spherical particles and an average Rh atom area of 7.9×10^{-20} m^2 (*32*) yielded an average particle size of 10 nm, in good agreement with a value of 11 nm determined by XRD line broadening analysis using the Scherrer formula (*33*). The catalyst loading was measured by atomic absorption following the procedure described in (*34*).

Reactor-flow system. A once-through stainless steel microreactor of 0.5 ml inter-

nal volume was used in all the transient and steady-state experiments. Its behavior as a true CSTR was previously reported (*12, 13*). The integrity of the transient results, free of any flow disturbances, was maintained as described (*11, 35*). H_2/CO mixtures were prepared based on 9.9% CO and the appropriate H_2 composition to give the stated ratio with He as a balance. The flow rate of all gases used was 30 ml/min (ambient). At this flow rate the mean residence time in the reactor (0.5 ml) was 1 s. The He gas used was UHP, and the H_2 standard (99.98%). Further purification of these gases was performed as previously described (*12, 13*).

Mass spectrometry. The high resolution mass spectrometer (Nuclide 12-90-G), tuned-up properly, produced flat-topped peaks for all the mass numbers studied. Sensitivity and cracking patterns of components were recorded before and after each transient run. Results were obtained with a MINC-11 microcomputer (DEC) from an electron multiplier/electrometer system ($\tau = 0.1$ s). Data acquisition and calibration against dilute mixtures were performed at the same data acquisition frequency. To improve on the statistical noise and have a high signal-to-noise ratio, 200 pts were collected at the frequency of 1 kHz and the average value was stored. Three averaged data values every second were enough to follow all the transients of one mass number at a time. Several mass numbers were scanned when appropriate, yielding 2 mass numbers s^{-1}. Methane transients were recorded at $m/e = 15$. Under the ion source conditions set for the mass spectrometer and according to the product distribution, C_2^+ contribution to $m/e = 15$ was less than 2%. Pure ethane transients were obtained by using the $m/e = 30$ in certain experiments. Other mass numbers used were 18, 28, 29, 40, 44 for H_2O, $^{12}C^{16}O$, C_3 and $^{13}C^{16}O$, Ar, and CO_2 components.

Gas chromatography. Steady-state product distribution was obtained by using a GC (CARLE 311) with a 1.8 m × 2 mm stainless steel column packed with Chromosorb 102 and an H_2 flow rate of about 25 ml/min. The flame ionization detector (FID) was exclusively used except for H_2O. The measure of CO_2 was made by using the FID after passing the effluent from the column through a hydrogenolysis reactor (*13*). The CO/H_2/H_2O mixture was produced by passing the CO/H_2 feed through a saturator of distilled water held at room temperature. Known dilute mixtures of hydrocarbons were prepared for calibration purposes. For the chromatographic separation, CO, CH_4, and CO_2 were separated at 45°C. The column then was programed at 8°C/min to 180°C for rapid and complete resolution of the other products. However, an overlapping of about 20–30% for the C_4^+ products between the paraffinic and olefinic components was present. No attempts were made to resolve them completely. A complete GC analysis run as described above required about 17 min. GC peaks were measured with the microcomputer at the rate of 5 pts/s. Integration was done by using the trapezoidal rule.

RESULTS

Steady-State Experiments

The activity and selectivity of the CO/H_2 reaction over the 5% Rh/Al_2O_3 catalyst have been studied at atmospheric pressure and at temperatures in the range 240–285°C. Some results are shown in Table 1 for H_2/CO = 9 and 3 h on stream. The main product is always methane; there is very little methanol formed (30–60 ppm) and less than 10 ppm of ethanol and acetaldehyde are found. The CH_4 selectivity shown at 240°C is similar to that reported at 180°C, where only CH_4, H_2O, and small quantities of C_2H_6 and CO_2 were measured (*11*). As seen from the last column in Table 1, the conversion is small enough so that initial rates are obtained. To approximate the effect of higher conversion on the reaction, water was added to the feed as shown. Selectivity toward CH_4 is generally increased,

TABLE 1

Activity and Selectivity of a 5.2% Rh/Al_2O_3 Catalyst during Synthesis Gas Reaction. Effect of H_2O on Product Selectivity[a]

T (°C)	$C_2^=/C_2$		$C_3^=/C_3$		S_{CH_4} (%)[b]		S_{CO_2} (%)		S_{MeOH} (%)[b]		α[c]		X_{CO} (%)[d]	
240	0.210[e]	0.270[f]	2.20	2.70	72.0	79.0	1.2	4.0	2.0	1.85	0.45	0.41	1.7	1.63
255	0.140	0.187	1.45	2.00	80.0	81.0	1.54	3.4	1.10	1.00	0.41	0.39	3.65	2.10
270	0.085	0.100	1.00	1.12	87.0	84.6	1.85	3.70	0.52	0.40	0.39	0.37	5.8	5.05
285	0.054	0.058	0.58	0.60	90.0	87.3	2.20	4.78	0.26	0.17	0.37	0.37	9.4	7.50

[a] Selectivity is defined as $S = Iy_I/\sum Ny_N \times 100\%$, where, y_I = mole fraction of a product in the gas phase with I carbon atoms and y_N = mole fraction of a product in the gas phase with N carbon atoms.

[b] Not including CO_2.

[c] Based on C_3–C_6.

[d] Not including CO_2; $X_{CO} = \sum Ny_N/y^f_{CO} \times 100\%$, where y^f_{CO} is the mole fraction of CO in the feed stream.

[e] First column corresponds to $H_2/CO = 9$.

[f] Second column corresponds to 1.7% H_2O in $H_2/CO = 9$ feed.

although for temperatures higher than 255°C it is decreased. The selectivity toward CO_2 shows some increase and the activity is reduced. However, these effects are small.

As shown by Figs. 1A and B, the effect of time on stream on the product composition and reaction rate is modest, accounting for not more than a 25% deactivation over 3 h. All the rates decrease together, approximately, so that the selectivities at times less than 3 h remain close to those of Table 1. The activation energy of the methanation reaction obtained from Fig. 1C is 22.7 kcal mol^{-1}, in agreement with previous results for both Rh and other metals (*9, 22, 36, 37*). The presence of water in the reacting gases has little effect on the activation energy (E = 23.4 kcal mol^{-1}), but a greater effect on the methanation rate, as illustrated by Fig. 1C.

Changes in selectivities are affected much more by the H_2/CO ratio than by temperature or time on stream, as can be deduced from Figs. 2A and B. The changes are in the expected directions, as reflected by the variation in the H/CH_x ratio on the metal surface as it is affected by the H_2/CO ratio in the gas phase. This ratio also has a large effect on reaction rates, as illustrated by Fig. 2C. To keep the experimental program within reasonable limits, we did not vary the CO partial pressure.

Transient Experiments

The rest of this study will be devoted to various transient studies with the goal of measuring the surface composition of the catalyst under the various conditions which lead to the pseudo-steady-state results of Table 1 and Figs. 1 and 2. The most straightforward transient results are summarized in Figs. 3–6. In the isothermal experiment of Fig. 3 there is an initial transient as the reaction starts from a practically clean surface, followed by a period of pseudo-steady-state, followed by a second transient which corresponds to the titration of the surface with H_2. Much information is contained in the peak heights and shapes, and in the areas under the curves. In this paper we use these results to estimate the composition of the working surface and to comment on the kinetics in a qualitative way. Their complete exploitation via the confrontation of the experimental curves and those simulated by computer through a model based on the sequence of elementary steps remains an ultimate goal but beyond the scope of this report. All the

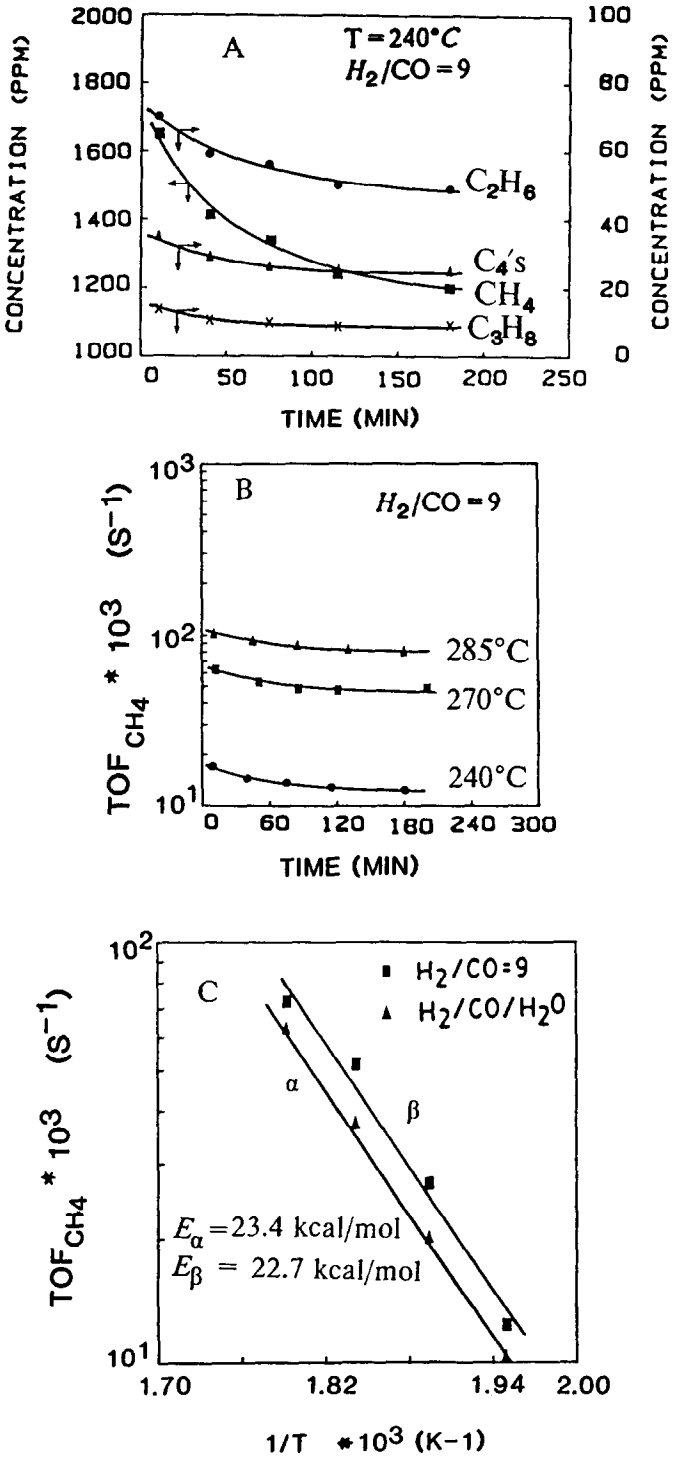

FIG. 1. (A) Product distribution vs time. C_4's include the olefins, both 1-$C_4^=$ and 2-$C_4^=$ and the paraffin n-C_4. (B) methane turnover frequency vs time. It is based on H_2 chemisorption result. (C) Arrhenius plot for methane turnover frequency with $H_2/CO = 9$ with and without H_2O in the feed.

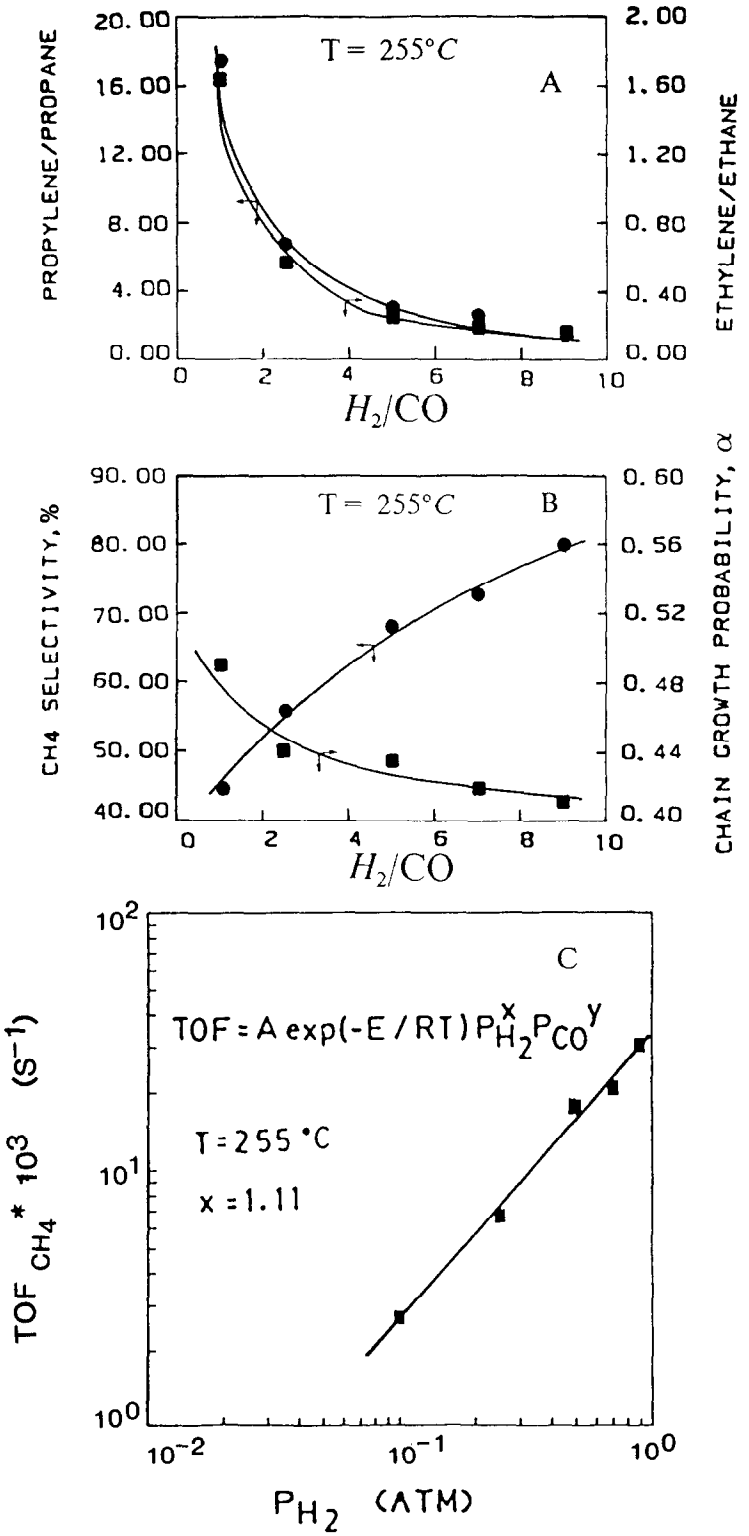

FIG. 2. (A) Effect of H_2/CO ratio on olefin/paraffin ratio for C_2 and C_3, $P_{CO} = 0.1$ atm, $T = 255°C$. (B) Effect of H_2/CO ratio on CH_4 selectivity and chain growth probability, $P_{CO} = 0.1$ atm, $T = 255°C$. (C) CH_4 turnover frequency dependency on H_2 pressure, $P_{CO} = 0.1$ atm, $T = 255°C$. All for 3 h on stream.

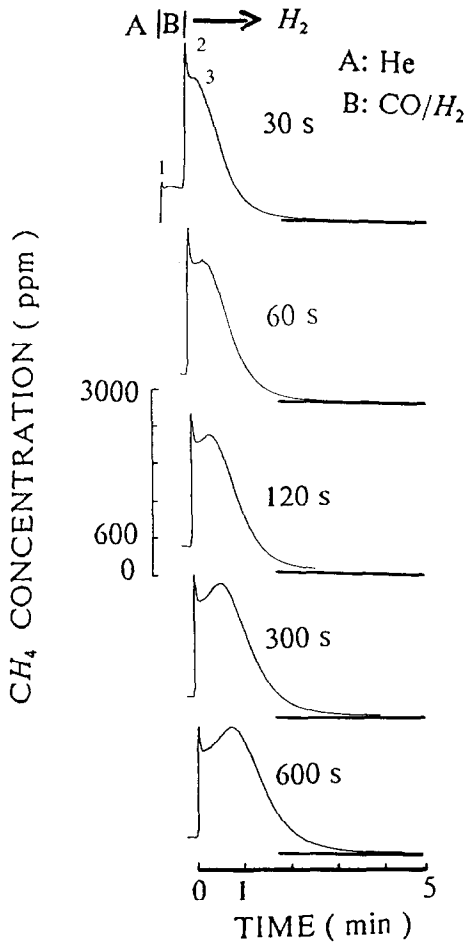

FIG. 3. Transient response of CH_4 at T = 200°C and H_2/CO = 9 according to the delivery sequence: He(180 s) → $H_2/CO(\Delta t)$ → $H_2(t)$.

results are available on magnetic tape (*38*). All the transient studies are done on 30 mg of the supported catalyst using a constant gas flow rate of 30 ml/min in the differential/CSTR reactor as already described.

The first sharp peak in the top curves of Figs. 3–6 occurs as H_2/CO starts to flow over the catalyst. It is designated as peak 1 in Figs. 3–6, and it grows with temperature as shown in Fig. 7. In Figs. 3–6, peak 1 is shown only for the top graph (Δt = 30 s). It is of course identical for the lower graphs ($\Delta t > 30$ s), but it is not visible since it is off scale to the left. A switch to H_2 at Δt then produces the sharp peak 2 as defined in Figs. 3–6 which grows with temperature and diminishes with time on stream (Fig. 7).

For short times on stream ($\Delta t \leq 120$ s) the isothermal titration in H_2 removes almost all the surface carbon-containing species within a few minutes (Figs. 3–6). At 200°C this is true out to Δt = 600 s (Fig. 3). However, at higher temperatures (Figs. 4–6) less reactive carbon-containing species start to accumulate, and it is convenient to remove and measure them by programing the temperature in H_2 after the isothermal titration, as shown in the bottom graphs of Figs. 4–6. The broad peak obtained is called peak 4, as indicated in Figs. 4–6. The less reactive species accumulate with time on stream and grow faster as the temperature is increased. The area under the titration peaks (2, 3, and 4 in Fig. 4, for example) furnishes the surface coverage of the sum of all the surface carbonaceous species, and these are reported in Table 2. Eventually we shall be able to identify in some detail the surface components which contribute to these peaks.

We turn our attention now to the CH_4 peaks formed under the isothermal titration of the surface by H_2. This process usually produces two peaks, designated as peak 2 and peak 3 in Figs. 3–5. Peak 3 grows with time on stream with respect to peak 2, as shown in Figs. 3–5. In fact, at 30 s time on stream and 240°C only peak 2 is discernable

TABLE 2

Total Coverage of Surface Carbon-Containing Species Isothermally Hydrogenated to CH_4 (Peaks 2 and 3)

Time on stream in H_2/CO (s)	T = 200°C	T = 220°C	T = 240°C	T = 260°C
30	1.47	1.53	1.28	1.38
60	1.72	—[a]	—[a]	—[a]
120	1.80	1.82	1.55	1.50
300	2.10	—[a]	1.74	1.61
600	2.35	2.17	1.84	1.71
600[b]	—[a]	—[a]	3.68	3.68
3600	—[a]	2.00	—[a]	1.62
3600[b]	—[a]	3.48	—[a]	5.94

[a] Not measured.
[b] Quantities include the H_2 TPR, peak 4.

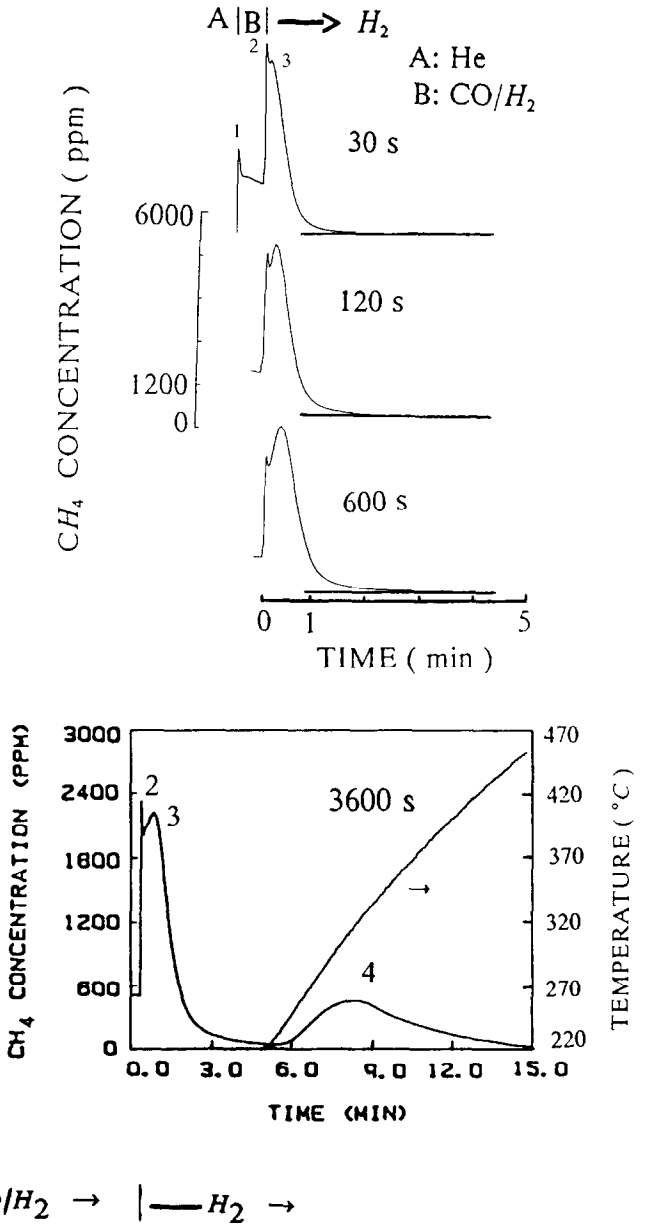

FIG. 4. Transient response of CH_4 at T = 220°C and H_2/CO = 9 according to the delivery sequence: He(180 s) → $H_2/CO(\Delta t)$ → $H_2(t)$. For Δt = 3600 s, after the isothermal H_2 reduction T is increased as shown. The numbering system for identifying the peaks is shown. Peak 1: that obtained at the start of reaction, He → H_2/CO; peak 2: first spike obtained after reaction for time Δt, caused by the switch CO/H_2 → H_2 followed by isothermal hydrogenation; peak 3: broad peak obtained after peak 2, caused by hydrogenation after a time Δt in H_2/CO; peak 4: peak(s) obtained by temperature programmed exposure to H_2 after the completion of the isothermal hydrogenation.

in Fig. 5. However, peak 3 appears at longer times on stream in H_2/CO. At 260°C, peak 3 is not visible at all (Fig. 6). At 220°C, peak 3 becomes higher than peak 2, a feature that has not been observed at other temperatures. As it grows with time on stream peak 3 takes longer to reach its maximum, and this behavior is summarized in

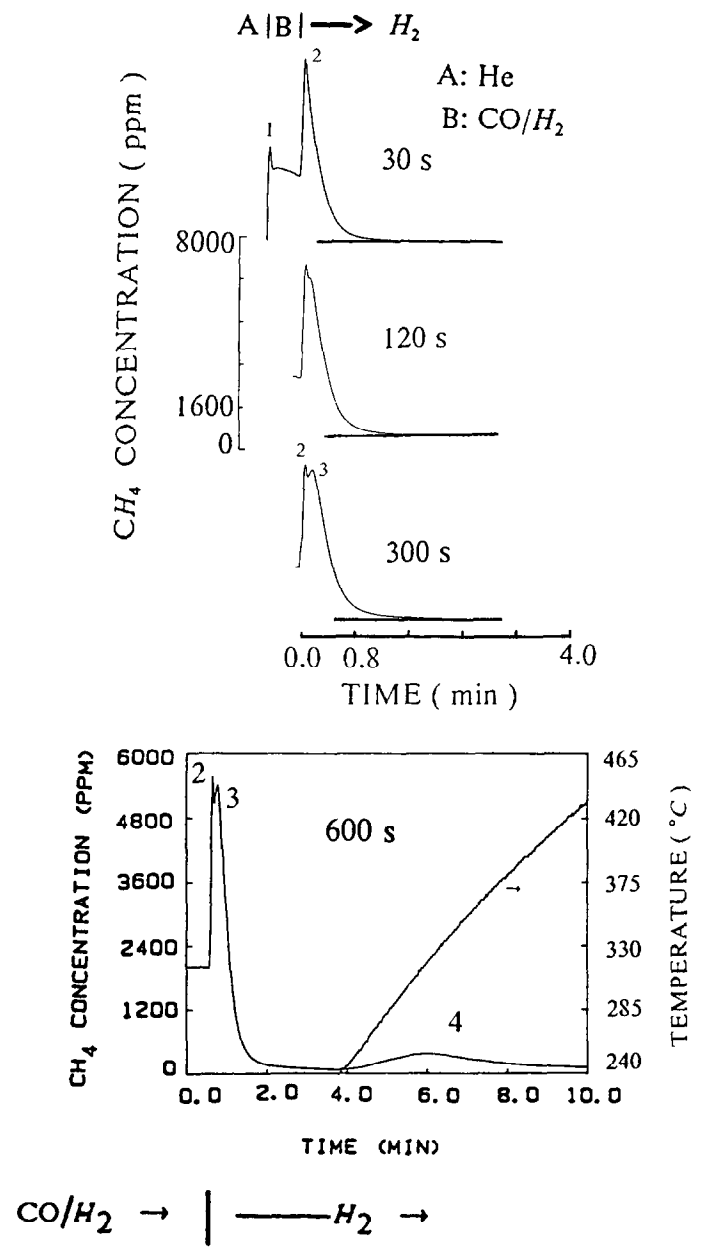

FIG. 5. Transient response of CH_4 at $T = 240°C$ and $H_2/CO = 9$ according to the delivery sequence: He(180s) → $H_2/CO(\Delta t)$ → $H_2(t)$. For $\Delta t = 600$ s, after the isothermal H_2 reduction T is increased as shown.

Table 3. Of course, as the temperature rises the peaks elute more quickly.

As the methane peaks of Figs. 3–6 are being formed, small concentrations of higher hydrocarbons may also form. Figure 8 shows the result for ethane at 240°C and 120 s on stream. The height of the ethane peak is 10^{-3} times that of methane peak 2 (Figs. 5 and 7). The areas under the peaks of Fig. 8 correspond to $\theta = 0.005$ at 120 s, 0.009 at 600 s, and 0.020 (total) at 1200 s. We should mention here that these tran-

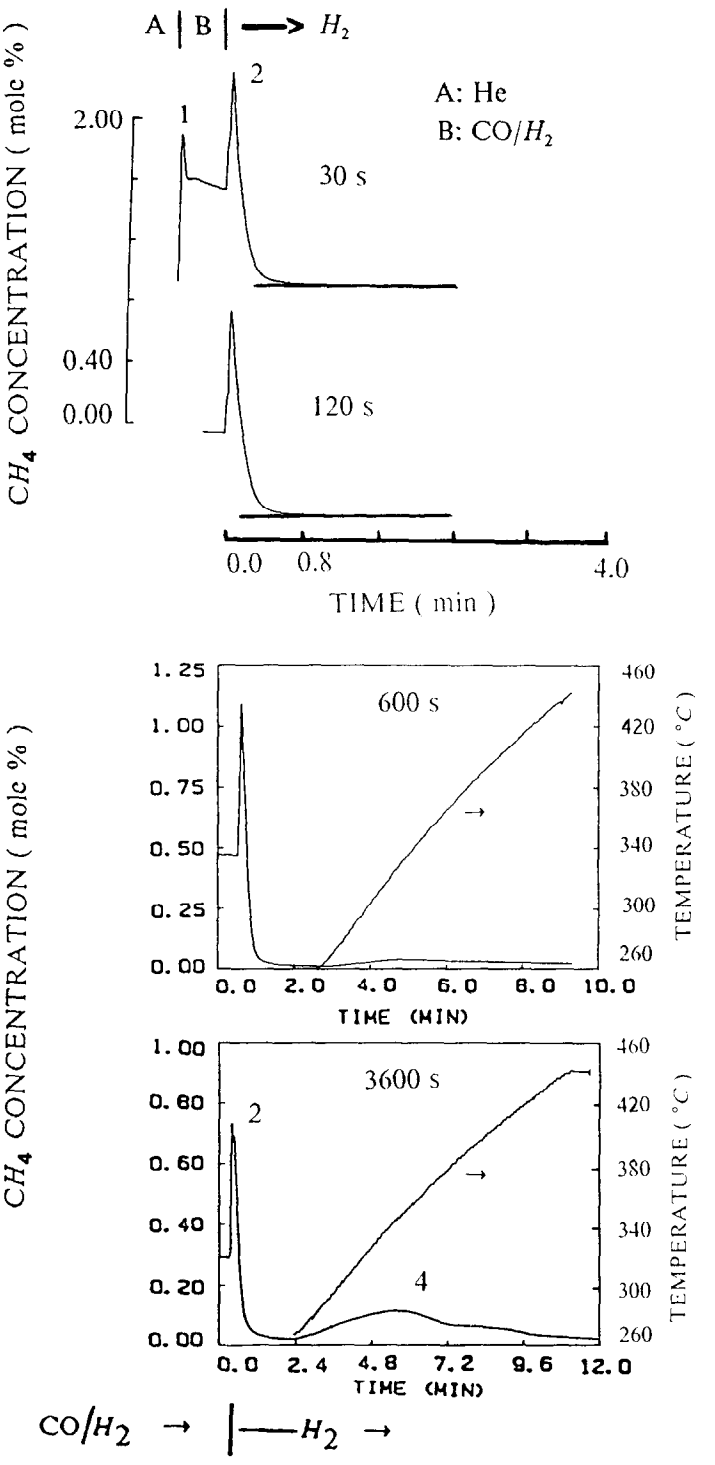

FIG. 6. Transient response of CH_4 at T = 260°C and H_2/CO = 9 according to the delivery sequence: He(180 s) → $H_2/CO(\Delta t)$ → $H_2(t)$. For Δt = 600 and 3600 s, after the isothermal H_2 reduction T is increased as shown.

TABLE 3

Time of Appearance[a] of Peak 3 Maximum under H_2 According to the Sequence: He(180 s) → $CO/H_2(\Delta t)$ → $H_2(t)$

Time on stream in H_2/CO Δt (s)	Time on stream in $H_2(t)$ (s)			
	T = 180°C	T = 200°C	T = 220°C	T = 240°C
30	—[b]	9	5	—[b]
60	48	16	—[c]	—[c]
120	60	22	10	4
300	88	33	—[c]	6
600	118	42	16	8
3600	185	—[c]	26	—[c]

[a] The zero time is considered that at the switch to H_2.
[b] No peak maximum has been observed.
[c] Data were not obtained.

sients were obtained based on m/e = 30, where no contribution from any other compounds was present.

Now we need to consider what is the source of peaks 2 and 3 under the hydrogen titration of Figs. 3–5. By analogy to previous studies on Ni (*39*) and on Ru (*40, 41*), it seems probable that the first extremely sharp peak 2 arises from the hydrogenation of a very reactive CH_x species on the surface (C_α), accumulated under CO/H_2, whereas peak 3 comes from adsorbed CO. However, for the Rh/Al_2O_3 catalyst there will be a contribution to peak 3 from formate on the support as will be illustrated in more detail by isotopic studies in Part II (*29*). To shed more light on this matter here the experiments shown in Fig. 9 were performed. Under CO/He it is expected that the Boudouard reaction will produce a peak of CO_2 (peak 5) as surface carbon is laid down on the Rh surface. The results of Fig. 9A show that the surface rapidly accumulates carbon, almost quenching the CO disproportionation at 200°C within 1 min. After this time a small production of CO_2 continues resulting in about 5 ppm of CO_2 in the product gas. The area under the peak up to 2 min gives θ_C = 0.06, a value far below a monolayer. A subsequent switch from CO/He to hydrogen produces a methane peak which does not give peak 3 found in Figs. 3–6, but instead a shoulder decaying with time in a fashion which depends on the temperature. The latter has been demonstrated in a previous report at 180°C (*11*) and for higher temperatures will be shown in Part II (*29*).

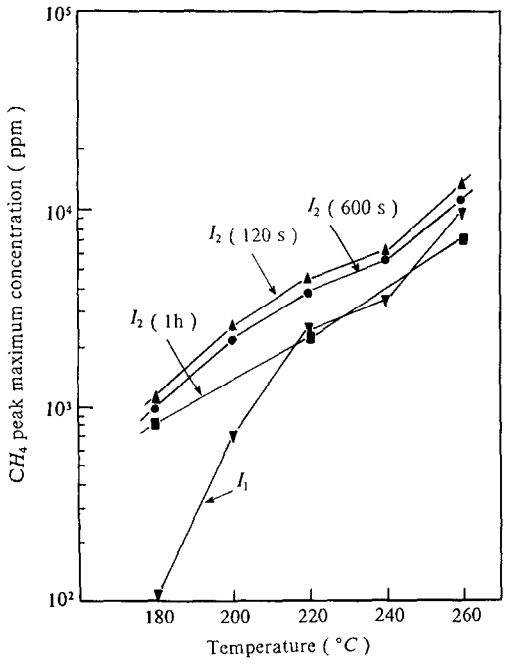

FIG. 7. CH_4 peak maximum concentration vs temperature under various times in CO/H_2. Delivery sequence: He(180 s) → $CO/H_2(\Delta t)$ → $H_2(t)$. I_1 = peak maximum under H_2/CO, I_2 = maximum of first peak (peak 2) under isothermal hydrogenation. Data at 180°C from (*11*).

We have found that the sharp peak and the shoulder referred to above can be separated by quenching the system in helium to 100°C. Very little CO, about 4% of an equivalent monolayer, desorbs during the cooling period (8 min from 200 to 100°C). Then the feed is switched to H_2 and the TPR of Fig. 9B is carried out. More details on this deconvolution procedure can be found elsewhere (*11*). Peak 2 yields θ_{C_α} = 0.044 and peak 3 θ_{CO} = 0.89. Since the TPR of CO adsorbed at temperatures up to 100°C yields only one symmetrical peak which reaches the base line at about 320°C, we define a relatively inactive carbon (C_β) as that which reacts above 350°C. This defi-

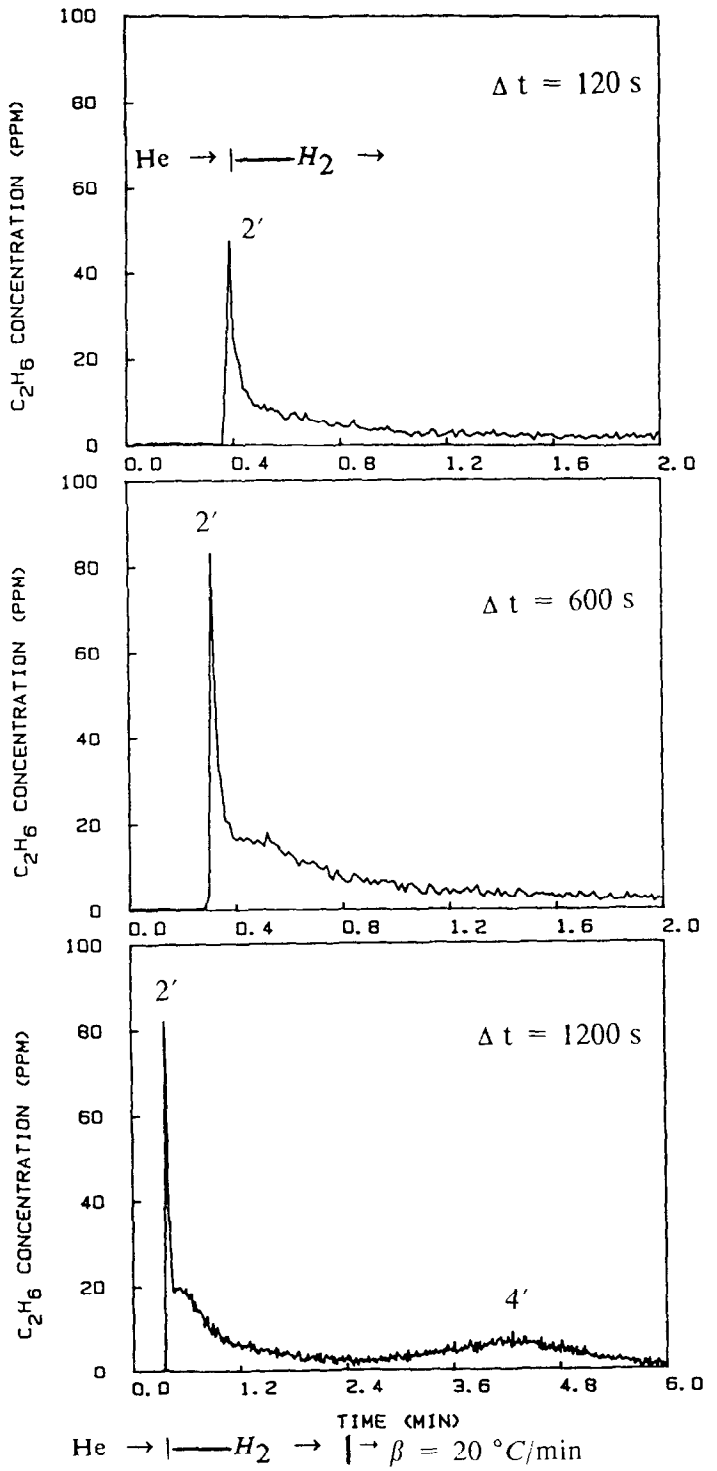

FIG. 8. Transient response of C_2H_6 at T = 240°C and H_2/CO = 9 according to the delivery sequence: He(180 s) → $H_2/CO(\Delta t)$ → He(120 s) → $H_2(t)$. For Δt = 1200 s, after the isothermal H_2 reduction T is increased as indicated.

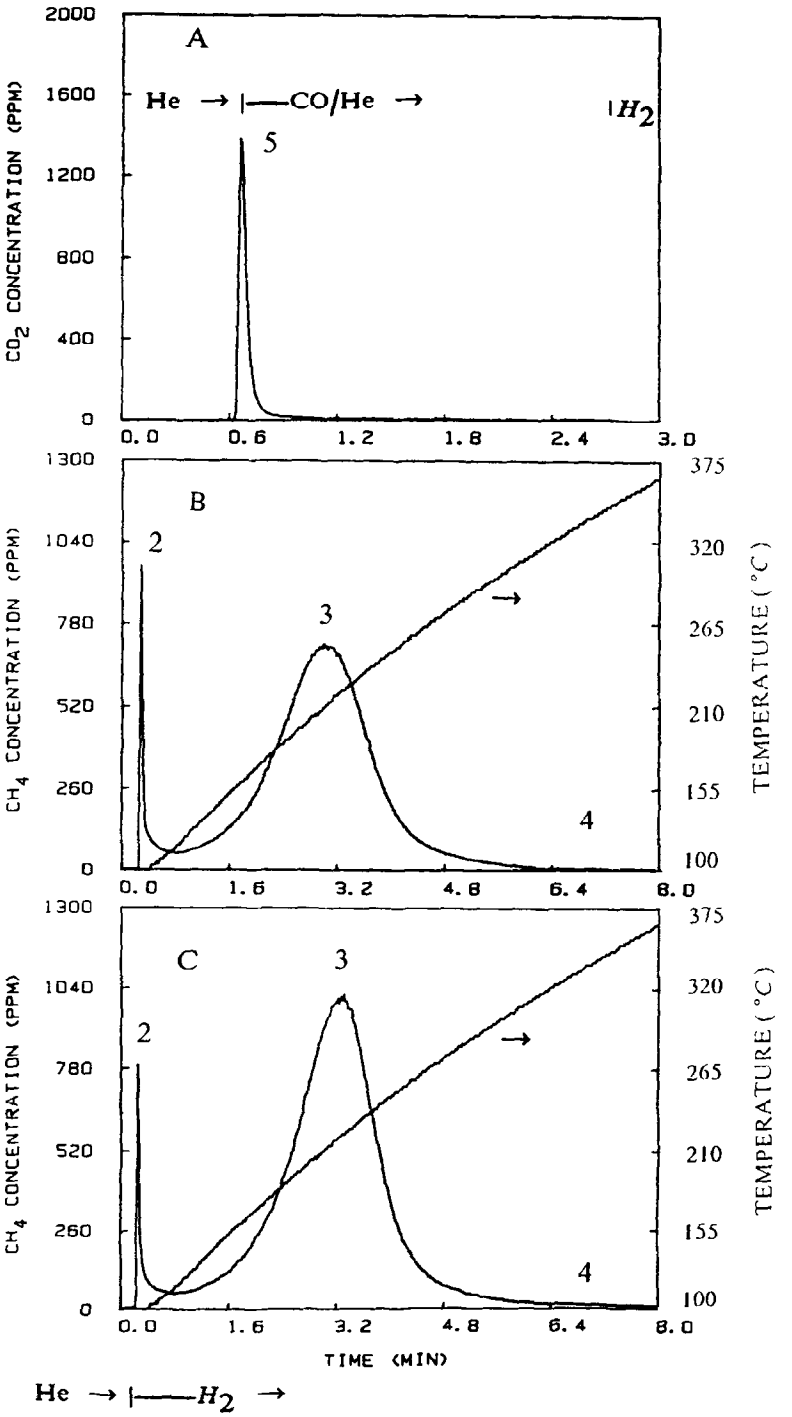

FIG. 9. (A) Transient response of CO_2 (peak 5) at T = 200°C according to the delivery sequence: He(180 s) → CO/He(120 s) → $H_2(t)$. (B) TPR response of CH_4 according to the delivery sequence: He(180 s) → CO/He (120 s), T = 200°C → He, cool-down to 100°C → $H_2(t)$; T is increased as shown. (C) TPR response of CH_4 according to the delivery sequence: He(180 s) → CO/H_2(120 s), T = 200°C → He, cool-down to 100°C → $H_2(t)$; T is increased as shown.

nition is arbitrary, as some C_β may be reacted off to form part of the peak attributed to CO. From Fig. 9B we find $\theta_{C_\beta} = 0.009$. We note that a small peak of ethane is also produced during the formation of the sharp methane peak 2. We should note the good agreement of the CO_2 transient (peak 5) ($\theta_c = 0.06$) with the deconvolution experiment of Fig. 9B ($\theta_{C_\alpha} + \theta_{C_\beta} = 0.053$) (peak 2 + peak 4).

When the same procedure as in Fig. 9B is applied after 2 min on stream in H_2/CO, the result of Fig. 9C is obtained. We estimate $\theta_{C_\alpha} = 0.04$ and $\theta_{C_\beta} = 0.014$. However, the θ from the large carbon-containing peak 3 is now 1.15 monolayers. This value indicates that there must be some other carbonaceous species in addition to CO* which contribute to this central peak. Following the work of Solymosi and his group (*9, 23*) we have already proposed that the other species is a formate located on the alumina support (*11*). The formate is reported to be reactive toward H_2 in the range of 170–350°C (*23*). This is the basis for our definition of the inactive carbon species C_β under CO/H_2, as that which is hydrogenated above 350°C. We note that formate apparently does not form on the Al_2O_3 in the CO/He mixture which leads to Fig. 9B or if it does form is not reactive toward hydrogen to give methane. Convincing evidence for the existence of the formate via infrared spectroscopy and TPR has been presented (*9, 23*). In a continuation of the present work we shall show that transient isotopic studies with ^{13}CO permit us to distinguish between the amount of adsorbed CO and the amount of formate, also giving support for the present assignment (*29*). However, here we base our reasoning on the nonisotopic methods described up to this point. Note that Table 2 shows total coverages of carbonaceous species to be consistently in excess of a monolayer under H_2/CO.

Figure 10 shows the same experiments as those in Fig. 9, but at 260°C. Note that peak 2 at 2 min in Fig. 6 is now nicely resolved into two peaks in Fig. 10C. In both Figs. 10B and C there is now a larger accumulation of C_β, because of the higher temperature. In the CO_2 transient (Fig. 10A), at the switch to H_2 there is a small but discernable peak of CO_2, absent at 200°C. The following coverages are obtained: Fig. 10A, $\theta_c = \theta_{C_\alpha} + \theta_{C_\beta} = 0.18$; Fig. 10B, $\theta_{C_\alpha} = 0.047$, $\theta_{CO} = 0.83$, $\theta_{C_\beta} = 0.123$; Fig. 10C, $\theta_{C_\alpha} = 0.024$, $\theta_{CO} + \theta_{COOH} = 1.03$, $\theta_{C_\beta} = 0.116$. A good agreement is observed between total carbon from the CO_2 transient with C_α and C_β from Fig. 10B. It is not excluded that some carbon reacted away at $T < 350$°C. Experiments like those of Figs. 9A and 10A have been performed out to higher temperatures, and it is found that large amounts of surface carbon may accumulate. Figure 11 shows the amounts of carbon calculated from the areas under peak 5 with its tail out to 2 min, as a function of temperature.

It is now possible to estimate the surface coverages on Rh/Al_2O_3 during reaction from the results described so far. Methane peak 1 is not related directly to a surface species, but its meaning will be considered in the discussion later on. Methane peak 2 represents the active carbon C_α. In Figs. 3–5 it is cofounded with peak 3, but in Figs. 9 and 10 it is nicely resolved from peak 3. Methane peak 3 in Figs. 9B and 10B represents the surface CO, obtained from CO/He. However, in Figs. 9C and 10C and in Figs. 3–6 it represents the CO on the Rh metal plus what we claim is a formate surface species on the Al_2O_3. This will also be discussed further later on. Methane peak 4 represents the inactive carbon-containing species C_β, which accumulate at relatively large times on stream and high temperatures. Peak 5 (CO_2) represents the carbon formed under CO/He, and it is about equal to $C_\alpha + C_\beta$ formed under short exposure time to CO/H_2. The sum of peaks 2, 3, and 4 represents all the carbon-containing species on the catalyst surface. This quantity is about equal to the sum of C_α, C_β, CO, and COOH (formate species), all present under reaction conditions. Thus the amount of formate can be estimated by difference.

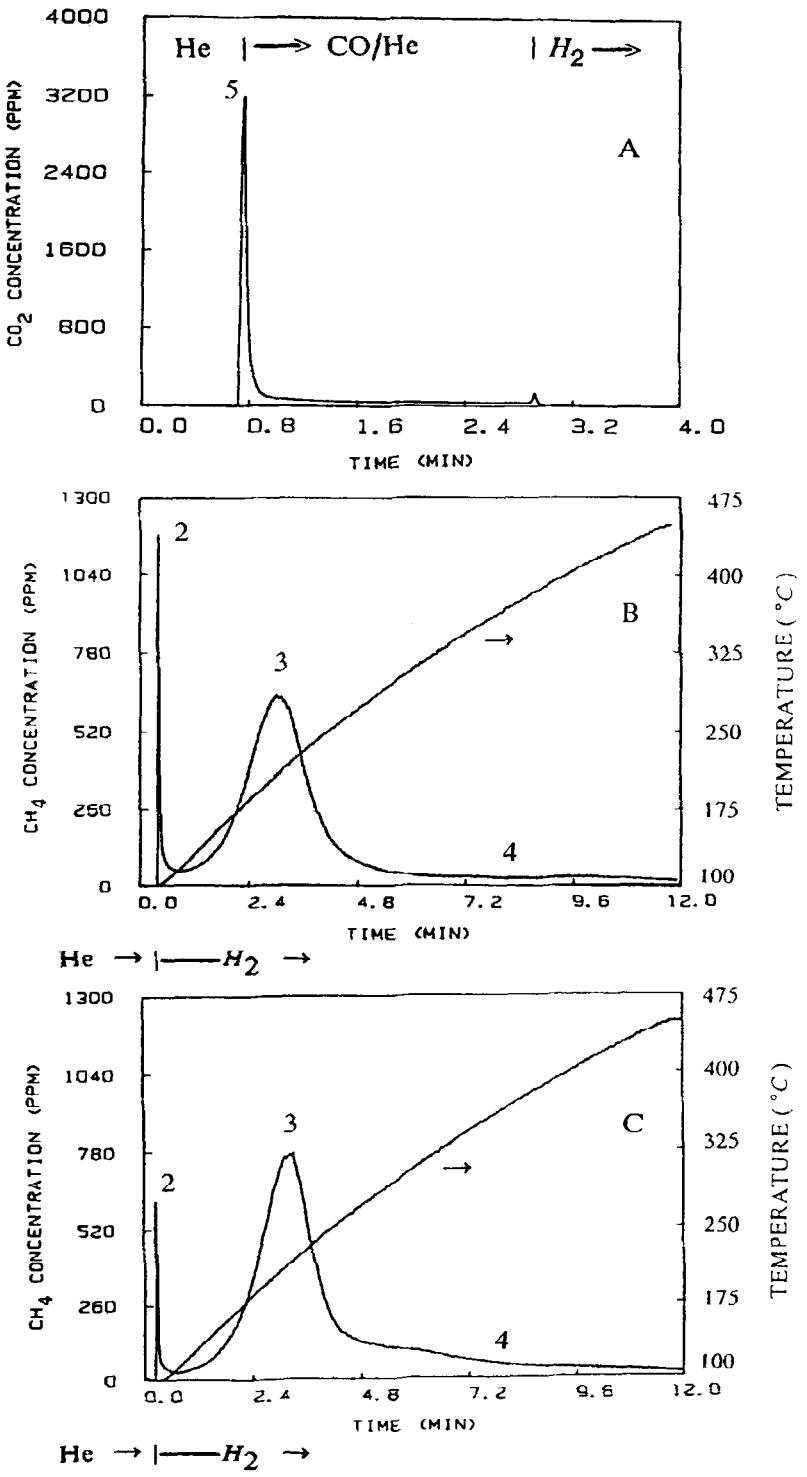

FIG. 10. (A) Transient response of CO_2 at T = 260°C according to the delivery sequence: He(180 s) → CO/He(120 s) → $H_2(t)$. (B) TPR response of CH_4 according to the delivery sequence: He(180 s) → CO/He(120 s), T = 260°C → He, cool-down to 100°C → $H_2(t)$; T is increased as shown. (C) TPR response of CH_4 according to the delivery sequence: He(180 s) → CO/H_2(120 s), T = 260°C → He, cool-down to 100°C → $H_2(t)$; T is increased as shown.

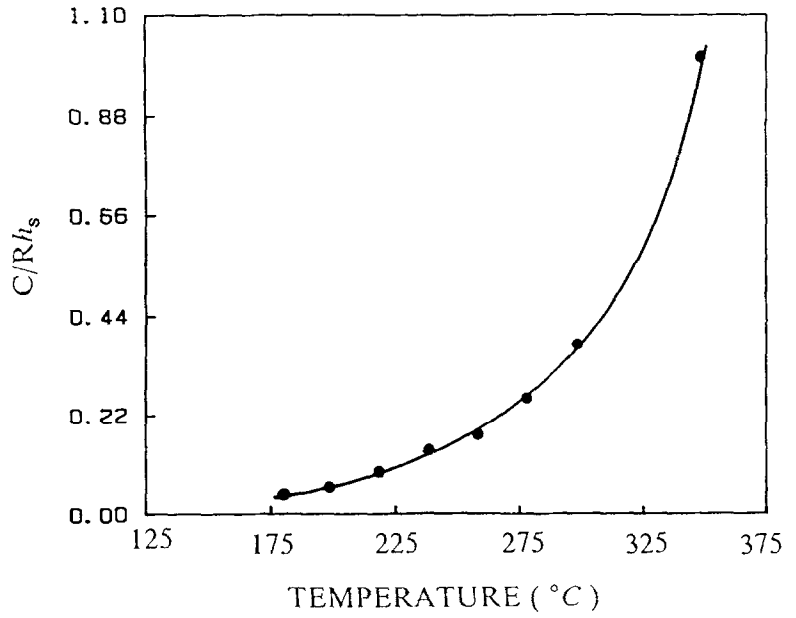

FIG. 11. Surface coverage of total carbon species (excluding CO) laid down by 2 min on stream in CO/He, as a function of temperature.

Following this scheme, Fig. 12 gives an overall view of the effect of temperature on the surface composition of the working catalyst after 2 min on stream in a reacting mixture of $H_2/CO = 9$ at 1 atm total pressure. The method of measuring the CO coverage from the CO/He experiment (Figs. 9B and 10B) has three weaknesses: (1) the coverage of CO may not be the same under CO/He and CO/H_2; (2) some CO may desorb in He as the system is cooled before the TPR, and during the H_2 titration; and (3) some less active carbon-containing species may react at $T < 350$°C. These matters will be studied further in Part II of this work (*29*).

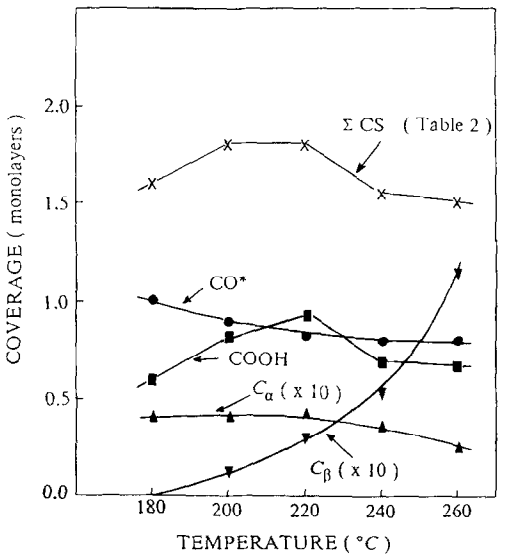

FIG. 12. Coverage vs temperature of the carbon-containing surface species present after 2 min in $H_2/CO = 9$ stream.

DISCUSSION

Steady-State Results

In general the selectivity of the 5% Rh/Al_2O_3 catalyst at 1 atm total pressure obtained in this study agrees with that previously reported on various Rh/Al_2O_3 catalysts (*8–10, 36, 49*). We have presented in this study a broad spectrum of data on the selectivity and activity of the 5% Rh/Al_2O_3 catalyst. Of interest are the high ratio of propylene/propane at low H_2/CO, and the absence of any measurable oxygenate product at $H_2/CO = 1$. The water–gas shift

reaction has been studied on Rh/Al_2O_3 catalyst, where an activation energy of 23 kcal mol^{-1} was obtained (*49*). This value is in agreement with that obtained in this study, if 1.7% H_2O is added to the $H_2/CO = 9$ feed. For their 1% Rh/Al_2O_3 and Rh/TiO_2 catalysts, Solymosi *et al.* (*9*) reported that the ratio of C_nH_x/CH_4 increases with time on stream for $H_2/CO = 3$ at 270°C. However, for the temperature range of 240–285°C and for $H_2/CO = 9$ we have found that C_nH_x/CH_4 remains constant.

Transient Results

The peak heights presented in Fig. 7 and the surface coverages corresponding to the various peaks as summarized in Fig. 12 permit us to reason about the sequence of steps for the CO/H_2 reaction. We can also come to qualitative conclusions about the relative rates of the steps, but in this paper no attempt is made to simulate the transient effects by a quantitative model. Let us now review what can be learned from the various peaks observed during the transient experiments.

Peaks 1 and 2. As for other metals, the high overshooting of peaks 1 and 2 in Figs. 3–6 is in agreement with the high surface coverage of carbonaceous species and the resulting exclusion of hydrogen from the surface (*13, 39, 40*). This also agrees with the reaction order of about unity with respect to hydrogen deduced from Fig. 2C. Although the surface coverage of C_α changes little with temperature (Fig. 12), its reactivity rises sharply with temperature (Fig. 7, I_2). Plotting the data of Fig. 7 (I_2, 120 s) vs $1/T$ gives a rough activation energy of 14.2 kcal mol^{-1} for the hydrogenation of C_α, compared to 26.4 kcal mol^{-1} for I_1. The latter is in a good agreement with the value obtained from steady-state results (Fig. 1C). In view of the high coverage of CO and the low coverage of C_α during reaction (Fig. 12) it is logical to think that the dissociation of surface CO is rate controlling and that the hydrogenation of C_α is rapid. Thus peak 1, formed during the initial H_2/CO reaction, may be expected to vary with temperature according to an activation energy similar to that of the overall reaction, as observed. It also follows that the activation energy for the hydrogenation of C_α (peak 2, no CO dissociation involved) should be lower than that associated with peak 1, as observed.

In attempting to understand the narrow peaks corresponding to I_1 and I_2 it is important to recall that the CSTR used here at a flow rate of 30 ml/min (ambient) has a response time of about 1 s (99% response in 5 s). Thus if the switch $He \rightarrow CO/H_2$ really produces a δ-function of CH_4, this will be observed as a peak with a linewidth consistent with the 1-s response time. In other words, during a time somewhat less than 1 s, there can exist concentration gradients within particles or across the metal surface. Since CO adsorbs almost instantaneously and saturates the Rh surface, it is plausible to visualize a front of adsorbed CO which travels in the tiny catalyst bed as CO is suddenly admitted (*42*). Because of the large excess of hydrogen, during the development of peak I_1 the rate of methane production is high until the CO and other surface species grow and reduce the surface hydrogen coverage to the low value typical of steady-state. The reverse occurs when CO is cut off to form the peak I_2. It should be pointed out that if the mixing time of the reactor were much larger than 1 s, the very narrow peak 2 would not be observable, leading to the conclusion that there is no C_α, as proposed by Mochida *et al.* (*22*).

The overshoot nature of both peaks I_1 and I_2 is related to the fact that the surface composition is rapidly changing during their development. The relatively low activation energy corresponding to peak I_2, as mentioned before, is a related phenomenon. This is a reason why it is important to check the results given here by isotopic experiments (*29*), which can give the surface coverages and reactivities during reaction without changing the overall chemical composition of the surface (*13, 43–46*).

Peak 3. From Figs. 3–5 and Table 2 it is clear that the size of peak 3 increases with time on stream. The surface coverage corresponding to this peak largely exceeds a monolayer. However, it is unlikely that the Rh surface can hold more than about one monolayer of CO. Support for this view is obtained from Figs. 9 and 10. Under CO/He the surface coverage of peak 3 is 0.9 in Fig. 9B and 1.15 in the Fig. 9C, for example. From these results it is clear that peak 3 arises from surface CO plus another surface carbon-containing species. From the results of Solymosi *et al.* (*9, 23*) we conclude that the extra component in peak 3 is a formate on the alumina support. In Part II of this study (*29*) we shall present support of this view based on isotopic studies.

The results given here show that Rh/Al_2O_3 behaves in the same general way as Ni/Al_2O_3 (*39*), Ru/Al_2O_3 (*41*), and Ru/SiO_2 (*40*) for the CO/H_2 reaction. There are formate bands present on Ni/Al_2O_3 (*12*), but the formate present does not give peak shapes and quantities like those observed on Rh/Al_2O_3. On Ni the value of θ_{CO} is in the order 0.3–0.4 (*12*). For Ru/Al_2O_3 there is a strong formate band in the infrared (*47*), but this is not considered to be the source of any of the C_β observed on this catalyst (*41*).

Peak 2′. Ethane and higher-molecular-weight hydrocarbon transients, using $H_2/CO = 3$ at 178°C, have been obtained for Ru/Al_2O_3 (*41*). These transients were obtained based on $m/e = 27$, and in addition to a sharp peak 2′, a distinct second peak (peak 3′, our notation) appeared growing with time and exceeding a monolayer value. We do not observe this growing peak on Rh/Al_2O_3. For the present work on Rh, it is interesting that the hydrogenation of CH_x from He/CO and also from H_2/CO gives a peak of ethane (Fig. 8) and similar sharp methane peaks (Figs. 9, 10). This may indicate that $x = 0$, a result similar to that obtained for Ru/SiO_2 (*51, 52*).

Peak 4. This peak corresponds to inactive carbonaceous species and increases greatly with time and at higher temperatures (Fig. 12). The reactor did not have any measurable catalytic activity, and only a small quantity of methane above 450°C might arise from the reduction of carbon on/in the reactor walls (*12*). However, the increase in θ_{C_β} is accompanied by only slight decreases in θ_{C_α} and θ_{CO}. Thus it seems probable that the gradual deactivation with time indicated by Fig. 2B arises from the exclusion of H from the surface by C_β rather than from the exclusion of C_α and/or CO.

Peak 5. The sharp spike from the initial reaction of CO/He in Figs. 9A and 10A is similar in quantity and shape to those arising from C_α in Figs. 9B, C and 10B, C. The observation that ethane can be made by hydrogenating this peak reinforces the above suggestion that $x = 0$. Again, such a peak was not observed by Mochida *et al.* (*22*).

CONCLUSIONS

Although the surface of Rh/Al_2O_3 during H_2/CO reaction in the range 180–260°C has a much higher coverage of CO than Ru, Ni, or Fe when used for the same reaction, it seems clear that the methanation reaction sequence for Rh also passes through an active surface carbon species C_α. As time on stream increases, inert C_β accumulates on the metal and a formate species forms on the support. These species do not contribute to the formation of methane at steady-state, although they can be hydrogenated by various isothermal and temperature programed procedures. The Boudouard reaction proceeds readily on Rh/Al_2O_3, producing both C_α and C_β. More support for these conclusions will be found in Part II (*29*), to follow.

ACKNOWLEDGMENTS

Support of this work was provided by the National Science Foundation through Grant CBT-8517158 and by the University of Connecticut Research Foundation.

REFERENCES

1. Van der Lee, G., Schuller, B., Post, H., Favre, T. L. F., and Ponec, V., *J. Catal.* **98,** 522 (1986).
2. Ichikawa, M., *Bull. Chem. Soc. Japan* **51**(8), 2268 (1978).

3. Underwood, R. P., and Bell, A. T., *Appl. Catal.* **21,** 157 (1986).
4. Orita, H., Naito, S., and Tamaru, K., *J. Catal.* **90,** 183 (1984).
5. Poels, E. K., Mangnus, P. J., and Ponec, V., *in* "Proceedings, 8th International Congress on Catalysis, Berlin, 1984," Vol. II. Dechema, Frankfurt-am-Main, 1984.
6. Van der Berg, F. G. A., Glezer, J. H. E., and Sachtler, W. M. H., *J. Catal.* **93,** 340 (1985).
7. Bastein, A. G. T. M., van der Boogert, W. J., Van der Lee, G., Luo, H., Schuller, B., and Ponec, V., *Appl. Catal.* **29,** 243 (1987).
8. Kuznetzov, V. L., Romanenko, A. V., Mudrakovskii, I. L., Matikhin, V. M., Shmachkov, V. A., and Yermakov, Y. I., *in* "Proceedings, 8th International Congress on Catalysis, Berlin, 1984," Vol. V. Dechema, Frankfurt-am-Main, 1984.
9. Solymosi, F., Tombacz, I., and Kocsis, M., *J. Catal.* **75,** 78 (1982).
10. Katzer, J. R., Sleight, A. W., Gajardo, P., Michel, J. B., Gleason, E. F., and McMillan, S., *J. Chem. Soc. Farad. Discuss.* **72,** 121 (1981).
11. Efstathiou, A. M., and Bennett, C. O., *Chem. Eng. Commun.* **83,** 129 (1989).
12. Stockwell, D. M., Chung, J. S., and Bennett, C. O., *J. Catal.* **112,** 135 (1988).
13. Stockwell, D. M., and Bennett, C. O., *J. Catal.* **110,** 354 (1988).
14. Erdohelyi, A., and Solymosi, F., *J. Catal.* **84,** 446 (1983).
15. Fujimoto, K., Kameyama, M., and Kunugi, T., *J. Catal.* **61,** 7 (1980).
16. Yates, J. T., Williams, E. D., and Weinberg, W. H., *Surf. Sci.* **115,** L93 (1982).
17. Solymosi, F., and Erdohelyi, *Surf. Sci.* **110,** L630 (1981).
18. Solymosi, F., and Pasztor, *J. Phys. Chem.* **89,** 4789 (1985).
19. Solymosi, F., and Pasztor, *J. Phys. Chem.* **90,** 5312 (1986).
20. Yang, A. C., and Garland, C. W., *J. Phys. Chem.* **61,** 1504 (1957).
21. Worley, S. D., Rice, C. A., Mattson, G. A., Curtis, C. W., Guin, J. A., and Tarrer, A. R., *J. Phys. Chem.* **86,** 2714 (1982).
22. Mochida, I., Ikeyama, N., Ishibashi, H., and Fujitsu, H., *J. Catal.* **110,** 159 (1988).
23. Solymosi, F., Bansagi, T., and Erdohelyi, *J. Catal.* **72,** 166 (1981).
24. Vis, J. C., Van't Blik, H. F. J., Huizinga, T., Van Grondelle, J., and Prins, R., *J. Catal.* **95,** 333 (1985).
25. Cairns, J. A., Baglin, J. E. E., Clark, G. J., and Ziegler, J. F., *J. Catal.* **83,** 301 (1983).
26. Nunez, G. M., Patrignani, A. R., and Rouco, A. J., *J. Catal.* **98,** 554 (1986).
27. Siddall, J. H., Miller, M. L., and Delgass, W. N., *Chem. Eng. Commun.* **83,** 261 (1989).
28. Gopal, P. G., Schneider, R. L., and Watters, K. L., *J. Catal.* **105,** 366 (1987).
29. Efstathiou, A. M., and Bennett, C. O., *J. Catal.* **120,** 137 (1989). [Part II]
30. Bertucco, A., and Bennett, C. O., *Appl. Catal.* **35,** 329 (1987).
31. Benson, J. E., and Boudart, M., *J. Catal.* **4,** 704 (1965).
32. Scholten, J. J. F., Pijpers, A. P., and Hustings, A. M. L., *Catal. Rev.-Sci. Eng.* **27**(1), 151 (1985).
33. Matyi, R. J., Schwartz, L. H., and Butt, J. B., *Catal. Rev.-Sci. Eng.* **29**(1), 41 (1987).
34. List, G. R., Friedrich, J. P., Kwolek, W. F., and Evans, C. D., *J. Amer. Oil Chem. Soc.* **50**(6), 210 (1973).
35. Bennett, C. O., *in* "Catalysis under Transient Conditions" (A. T. Bell and L. L. Hegedus, Eds.), Amer. Chem. Soc. Symposium Series, Vol. 178, p. 1. Amer. Chem. Soc., Washington, DC, 1982.
36. Vannice, M. A., *J. Catal.* **37,** 449 (1975).
37. Vannice, M. A., *J. Catal.* **37,** 462 (1975).
38. Efstathiou, A. M., Ph.D thesis, University of Connecticut, 1989.
39. Underwood, R. P., and Bennett, C. O., *J. Catal.* **86,** 245 (1984).
40. Cant, N. W., and Bell, A. T., *J. Catal.* **73,** 257 (1982).
41. Zhou, X., and Gulari, E., *J. Catal.* **105,** 499 (1987).
42. Delgass, W. N., personal communication.
43. Yang, C.-H., Soong, Y., and Biloen, P., *in* "Proceedings, 8th International Congress on Catalysis, Berlin, 1984," Vol. II, pp. 3–14. Dechema, Frankfurt-am-Main, 1984.
44. Happel, J., "Isotopic Assessment of Heterogeneous Catalysis." Academic Press, New York, 1986.
45. Mims, C. A., and McCandlish, L. E., *J. Phys. Chem.* **91**(4), 929 (1987).
46. Happel, J., Suzuki, I., Kokayeff, P., and Fthenakis, V., *J. Catal.* **65,** 59 (1980).
47. Dalla Betta, R. A., and Shelef, M., *J. Catal.* **48,** 111 (1977).
48. Stockwell, D. M., Bianchi, D., and Bennett, C. O., *J. Catal.* **113,** 13 (1988).
49. Van't Blik, H. F. J., Vis, J. C., Huizinga, T., and Prins, R., *Appl. Catal.* **19,** 405 (1985).
50. Dictor, R., *J. Catal.* **106,** 458 (1987).
51. Winslow, P., and Bell, A. T., *J. Catal.* **86,** 158 (1984).
52. Duncan, T. M., Winslow, P., and Bell, A. T., *J. Catal.* **93,** 1 (1985).